2.1 Fluctuating Polymers

The basic molecules of life (DNA, RNA, proteins, \cdots) are *hetero-polymers*, formed by the covalent bonding of a sequence of elementary units (nucleic acids, amino-acids) in long chains. A *homo-polymer*, as in many synthetic organic molecules, is constructed by joining $N \gg 1$ copies of the same monomer. A simple example is *polyethylene*,

$$|-CH_2-|_N \equiv \cdots - CH_2 - CH_2 - CH_2 - \cdots$$
.

The degree of polymerization, i.e. the the number of repeated units, can be quite large, ranging from a few hundred for proteins, 10^4-10^5 for polyethelene, to as big as 10^9 for some DNA. Typically the covalent bonds holding the polymer together are strong and cannot be broken at room temperature. There can, however, be flexibility in aligning/bending successive monomers, resulting in a large number of configurational degrees of freedom for polymers, indicating that a statistical description of the problem is fruitful. Such a statistical perspective is useful for describing general properties common to both synthetic and natural polymers. For example, at very high (not necessarily physiological) temperatures all polymers will be in a swollen (denatured) state to take maximum advantage of entropy. The heterogeneity of the sequence is irrelevant in such a phase, and we shall thus initially focus on the fluctuations of a homo-polymer.

2.1.1 Rotational isomers

Successive carbon–carbon bonds in the chain can be in different relative orientations, called rotational isomers. In polyethelene, the low energy trans conformation leads to a straight configuration of the molecule (albeit with zigzag alignment of bonds). There are two higher energy gauche states which cause a kink of angle of $2\pi/3$ between successive segments of the polymer. Assuming an energy difference Δ between the trans and gauche states, at a temperature T, the probabilities of these configurations are proportional to corresponding Boltzmann weights, as

$$\frac{\text{prob.}(g)}{\text{prob.}(t)} = 2e^{-\beta\Delta}, \quad \text{with} \quad \beta = \frac{1}{k_B T}.$$

For $(CH_2)^N$, Δ is quite small (roughly 500 cal/mole or 1/3 k_BT), and the polymer is very flexible at room temperature. For other polymers $\Delta > k_BT$, and gauche states with probability

$$p(g_{+}) = p(g_{-}) = \frac{e^{-\beta \Delta}}{1 + 2e^{-\beta \Delta}},$$

are relatively rare. A typical configuration then consists of long straight segments with few kinks. The probability of a straight segment of (exactly) n monomers decays exponentially as $p_t^n(1-p_t) \propto \exp(-n/\bar{n})$, where $p_t = 1 - 2p(g)$ is the probability of a trans bond, and

$$\bar{n} = -\frac{1}{\ln p_t} = \left(\ln\left[1 + 2e^{-\beta\Delta}\right]\right)^{-1}.$$
 (2.28)

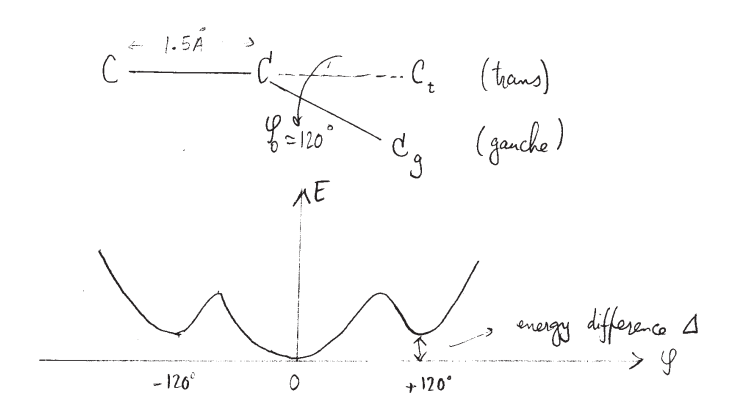


Figure 3: Trans–gauche configurations of a polymeric bond.

The average length of a straight segment is $a\langle n\rangle = ap_t/(1-p_t)$, where a is the bond length (monomer size). In the limit of $\beta\Delta\gg 1$, $\bar{n}\approx\langle n\rangle\approx e^{\beta\Delta}/2$.

The typical size of such straight segments is related to the *persistence* of the polymer. More precisely, the *persistence length* characterizes the exponential decay of orientational correlations along the chain. In the above simplified model, let us denote the orientation of the bonds by the set of vectors $\{\vec{t}_1, \vec{t}_2, \dots, \vec{t}_N\}$, with $\vec{t}_j \cdot \vec{t}_j = a^2$. Assuming that the (two) gauche states produce a relative bond angle ϕ , we have

$$\langle \vec{t_1} \cdot \vec{t_2} \rangle = a^2 \frac{1 + 2\cos\phi e^{-\beta\Delta}}{1 + 2e^{-\beta\Delta}} \approx a^2 \exp\left[-2(1 - \cos\phi)e^{-\beta\Delta}\right],$$

where the last expression is valid in the limit of $\beta \Delta \gg 1$ where a gauche state is very unlikely. In the same approximation, the correlation between bonds that are further apart is given by

$$\langle \vec{t}_1 \cdot \vec{t}_{n+1} \rangle \approx a^2 \frac{1 + 2n\cos\phi e^{-\beta\Delta} + \mathcal{O}(e^{-2\beta\Delta})}{1 + 2ne^{-\beta\Delta} + \mathcal{O}(e^{-2\beta\Delta})} \approx a^2 \exp\left[-2n(1-\cos\phi)e^{-\beta\Delta}\right],$$

where we have included only configurations with one gauche bond, contributions for additional gauche bonds are smaller by factors of $e^{-\beta\Delta}$. In this limit, the orientation correlations decay exponentially as $e^{-\ell/\xi_p}$, where $\ell=na$ is the counter-length along the polymer, and the persistence length ξ_p is given by

$$\xi_p \approx \frac{ae^{\beta\Delta}}{2(1-\cos\phi)}.\tag{2.29}$$

2.1.2 Worm-like chain

For a rigid polymer such as double-stranded DNA a kink causing a finite rotational angle is energetically costly and rare. The loss of angular correlations at long distances then occurs by accumulation of small changes from one monomer to the next. If we indicate as before a polymer configuration by the set of bond orientation vectors $\{\vec{u}_i \equiv \vec{t}_i/a\}$, we can approximate

the energy of a nearly straight configuration by

$$\mathcal{H} = -J \sum_{i=1}^{N-1} \vec{u}_i \cdot \vec{u}_{i+1} \,. \tag{2.30}$$

Since in a typical configuration \vec{t} changes slowly, it is useful to go over to a continuum limit in



Figure 4: The wormlike chain.

which the discrete monomer index i is replaced by the continuous arc-length $s \in [0, L = Na]$. Using $(\vec{u}_i - \vec{u}_{i+1})^2 = 2 - 2\vec{u}_i \cdot \vec{u}_{i+1}$, and replacing $\sum_{i=1}^{N-1}$ with $\int_o^L ds/a$, we obtain

$$\mathcal{H} \approx -JN + \frac{\kappa}{2} \int_0^L ds \left(\frac{d\vec{u}}{ds}\right)^2,$$
 (2.31)

where $\kappa = Ja$ is the coefficient of bending rigidity. (Note that $|d\vec{u}/ds| = 1/R(s)$, where R(s) is the local radius of curvature.)

Ignoring the initial energy of the "ground state" configuration, it is common to write the energy cost of bending in dimensionless form as

$$\beta \mathcal{H} = \frac{\xi_p}{2} \int_0^L ds \left(\frac{d\vec{u}}{ds}\right)^2 , \qquad (2.32)$$

with $\beta \kappa = \xi_p$. We have anticipated that the bending rigidity is related to the persistence length. In fact, it can be shown (e.g. by using transfer matrices) that for the discrete model of Eq. (2.30)

$$\langle \vec{u}_m \cdot \vec{u}_n \rangle \approx \left(\coth(\beta J) - \frac{1}{\beta J} \right)^{|m-n|} \quad \text{for} \quad |m-n| \gg 1,$$
 (2.33)

and thus in the continuum limit

$$\langle \vec{t}(s) \cdot \vec{t}(s+\ell) \rangle \approx a^2 e^{-\ell/\xi_p},$$
 (2.34)

with $\xi_p \approx \beta \kappa$ for $\beta J \gg 1$. This, so called *worm-like chain* model is frequently invoked as a description of double-stranded DNA, where ξ_p is in the range of 50–100nm.

2.1.3 Entropic elasticity

The flexibility of a long polymer arises from the statistical fluctuations of segments larger than the persistence length. The important parameter that governs the number of configurations is thus not the degree of polymerization N, but the number of unconstrained degrees

of freedom, or the Kuhn length $N_K \approx Na/(2\xi_p)$. To see this explicitly, let us consider the end to end separation of the polymer, given by

$$\vec{R} = \vec{t}_1 + \vec{t}_2 + \dots + \vec{t}_N = \sum_{i=1}^N \vec{t}_i$$
.

Because of rotational symmetry (there is no cost for rotating the entire polymer), $\langle \vec{R} \rangle = 0$, and its variance is given by

$$\langle R^2 \rangle = \sum_{i,j=1}^{N} \langle \vec{t_i} \cdot \vec{t_j} \rangle = Na^2 + 2 \sum_{i < j} \langle \vec{t_i} \cdot \vec{t_j} \rangle. \tag{2.35}$$

We shall assume that the orientational correlations decay as a simple exponential (this is only asymptotically correct), i.e.

$$\langle \vec{t}_i \cdot \vec{t}_j \rangle = a^2 e^{-a|i-j|/\xi_p} \,. \tag{2.36}$$

As the correlation function is the same for every pair of points separated by a distance k, and as there are (N - k) such pairs along the chain

$$\langle R^2 \rangle = Na^2 + 2a^2 \sum_{k=1}^{N} (N-k)e^{-ak/\xi_p}$$
 (2.37)

The above geometric series are easily summed, and for $N \gg 1$ (where only the term proportional to N is significant), we obtain

$$\langle R^2 \rangle = Na^2 \left(1 + \frac{2e^{-a/\xi_p}}{1 - e^{-a/\xi_p}} \right) = Na^2 \coth\left(\frac{a}{2\xi_p}\right)$$
 (2.38)

$$\approx 2Na\xi_p = (2\xi_p)^2 \left(\frac{Na}{2\xi_p}\right). \tag{2.39}$$

The approximations in the second line rely on $\xi_p \gg a$. The very last expression indicates that the behavior of the variance is the same as that of $N_K \equiv (Na/2\xi_p)$ independent segments of length $2\xi_p$, i.e. the same variance is obtained for a collection of N_K freely-jointed rods, each of length $2\xi_p$. Indeed the correlations between these Kuhn segments is sufficiently small that in the limit of $N_K \gg 1$, we expect the Central Limit Theorem to hold, leading to the probability distribution function

$$p(\vec{R}) = \exp\left[-\frac{3R^2}{2\langle R^2 \rangle}\right] \left(\frac{2\pi\langle R^2 \rangle}{3}\right)^{3/2} = \exp\left[-\frac{3R^2}{4Na\xi_p}\right] \frac{1}{(4\pi Na\xi_p/3)^{3/2}}.$$
 (2.40)

The final probability distribution is identical to the Boltzmann weight of a Hookian spring of strength $J_{polymer}$ connecting the end points of the polymer, and the result of entropic fluctuations can be interpreted as conferring an elastic bond between the ends of the polymer with spring coefficient

$$J_{polymer} = \frac{3k_B T}{\langle R^2 \rangle} = \frac{3k_B T}{2Na\xi_p}.$$
 (2.41)

2.2 Interacting Polymers

The polymeric properties discussed so far arose from the flexibility of the covalent bonds that join adjacent monomers. There are also interactions between any other pairs (triplets, etc.) of monomers which depend on their spatial vicinity and that favor certain spatial configurations. Indeed, it is such interactions, typically due to hydrogen bonds, that enable proteins to fold and assume specific shapes. There are competing effects due to thermal fluctuations and competition with solvent interactions.

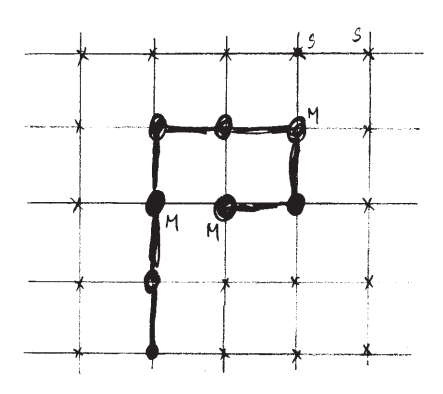


Figure 5: A self-avoiding walk on the square lattice.

Some of the ingredients of polymer interactions in a solvent are present in the very simple model of chain configurations on a (say square) lattice. The set of random walks on the square lattice that do not step back to the previous site grows with the number of steps N as 3^N . One simple consequence of interactions is that it is physically impossible to visit a previously occupied site. The steric constraint of excluded volume prunes the set of random walks to a smaller subset of so-called self-avoiding walks. The number of self-avoiding walks also grows exponentially as g^N with g < 3 ($g \approx 2.64$ for the square lattice).

A simple way to incorporate interactions on a lattice is to count the number of (non-polymeric) nearest-neighbor pairs, and assign energy

$$E = \epsilon_{mm} N_{mm} + \epsilon_{ms} N_{ms} + \epsilon_{ss} N_{ss} ,$$

where mm, ms, and ss stand for monomer-monomer, monomer-solvent, and solvent-solvent pairs respectively, with N_{pair} and ϵ_{pair} indicating the corresponding number and bond-energies. As two initially separate monomers are brought into contact, two ms bonds are replaced by one mm bond and one ss bond, leading to a change in energy of $\delta\epsilon = \epsilon_{mm} + \epsilon_{ss} - 2\epsilon_{ms}$. The preference of the monomers to aggregate in solvent is thus captured by the dimensionless "Flory–Huggins" parameter

$$\chi \equiv -\frac{\beta}{2}\delta\epsilon = \beta \left(\epsilon_{ms} - \frac{\epsilon_{mm} + \epsilon_{ss}}{2}\right), \qquad (2.42)$$

with the total energy expressed as ¹

$$E = E_0(\mathcal{N}, N) - 2k_B T \chi N_{mm}. \tag{2.43}$$

A negative χ leads to separation of monomers, while a positive χ encourages their aggregation. In a more realistic model, the interactions between molecules vary continuously as a

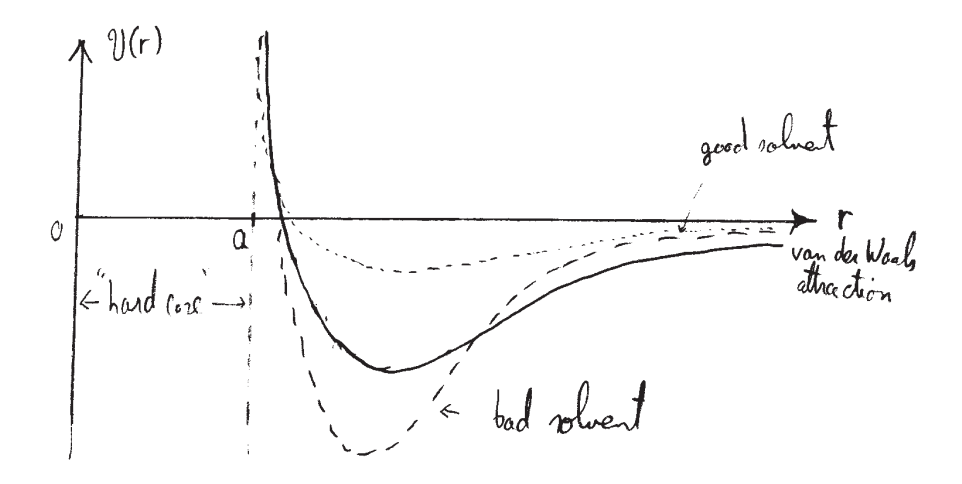


Figure 6: Effective interaction between monomers in a solvent.

function of their relative separation and orientation in space. The dependence on orientation is particularly relevant to hydrogen bonding, while the van der Waals attraction mainly depends on the separation. Just as in Eq. (2.8), an effective potential $\mathcal{V}(r)$ between monomers is in principle obtained by integrating over all positions (and orientations) of the solvent particles. In the usual case where the monomers are larger than the solvent molecules, the effective potential is attractive at large distances and has a hard repulsive core at short distances. For a good solvent the potential is weak, while a strong attractive potential favors aggregation of monomers in a bad solvent. The quality of solvent also changes as a function of temprature due to entropic contributions of its constituents. The larger entropy of solvent molecules typically improves the quality of a solvent at higher temperatures.

$$\mathcal{N} = N + N_{ss} + N_{sm} + N_{mm}.$$

On a lattice of coordination number z bonds per site, the (z-2)N non-=polymeric bonds adjacent to a polymer of length N are proportioned as

$$(z-2)N = N_{ms} + 2M_{mm}$$

as each monomer-monomer bond connects two sites. Substituting for N_{ss} and N_{ms} from the above two constraints reduces the expression for energy to

$$E = (\mathcal{N} - N)\epsilon_{ss} + (z - 2)N(\epsilon_{ms} - \epsilon_{ss}) + N_{mm}(\epsilon_{mm} - 2\epsilon_{ms} + \epsilon_{ss}) = E_0(\mathcal{N}, N) - 2k_B T \chi N_{mm}.$$

 $^{^{1}}$ As the total number \mathcal{N} of lattice bonds is divided amongst polymeric and non-polymeric bonds,

2.2.1 Mean-field estimate of the partition function

To calculate the properties of a polymer in solvent—e.g. to determine if it is in its native form or a denatured state at some temperature—we need to compute the free energy of the molecule and it environment. Computation of the partition function is a hard task, even for the highly simplified models we have introduced so far. We shall instead rely upon an approximate expression obtained in a mean-field/variational treatment. Let us assume that the most likely configurations of an interacting homopolymer have a typical size R. The partition function of N monomers confined to a sphere of radius R is then estimated as

$$Z(N,R) \approx g^{N} \times \frac{\exp\left(-\frac{3R^{2}}{4Na\xi_{p}}\right)}{(4\pi Na\xi_{p}/3)^{3/2}} \times \left\{1 \cdot \left[1 - \left(\frac{a}{R}\right)^{3}\right] \cdot \left[1 - 2\left(\frac{a}{R}\right)^{3}\right] \cdots \left[1 - (N-1)\left(\frac{a}{R}\right)^{3}\right]\right\} \times e^{-\beta E_{att.}}.$$
(2.44)

The first line in Eq. (2.45) pertains to the entropy of the polymer, the first term encodes the exponential growth in the number of configurations of an unconstrained polymer—the precise value of g is in fact irrelevant to the considerations that follow. The second term approximates the reduction in the number of configurations when the polymer is constrained to a size R. The effect of this reduction is included as a Hookian spring, motivated by the result in Eq. (2.40) for the end-to-end probability of a non-interacting polymer.

The second line in Eq. (2.45) approximates the effect of interactions and is broken into two parts. The first part encodes the reduction in phase space due to excluded volume constraints: the first monomer is unconstrained, the volume available to the second is reduced by the fraction $(a/R)^3$ due to the volume excluded by the first, and so on. The reductions due to the excluded volume make a contribution to the free energy proportional to

$$\delta \ln Z_{EV} = \sum_{i=1}^{N-1} \ln \left[1 - i \left(\frac{a}{R} \right)^3 \right] \approx - \left(\frac{a}{R} \right)^3 \sum_{i=1}^{N} i - \frac{1}{2} \left(\frac{a}{R} \right)^6 \sum_{i=1}^{N} i^2 + \cdots$$

$$\approx -\frac{N^2}{2} \left(\frac{a}{R} \right)^3 - \frac{N^3}{6} \left(\frac{a}{R} \right)^6 - \cdots$$
(2.45)

The attractive part of the interaction, for homopolymers, is given by

$$E_{att.} = \frac{1}{2} \sum_{i \neq j} \mathcal{V}(\vec{r}_i - \vec{r}_j) = \frac{1}{2} \int d^3 \vec{r} d^3 \vec{r}' n(\vec{r}) n(\vec{r}') \mathcal{V}(\vec{r} - \vec{r}').$$
 (2.46)

Assuming a uniform mean-density, $n(\vec{r}) = n = N/V = N/(4\pi R^3/3)$, leads to

$$E_{att.} = \frac{n^2}{2} V \int_a d^3 \vec{r} \mathcal{V}(\vec{r}) , \qquad (2.47)$$

where we have integrated over the center of mass of the pair to get the volume V, and ignored any contributions from the surface. In the spirit of Flory-Huggins, we introduce a

dimensionless parameter χ , via

$$\int_{a} d^{3} \vec{r} \mathcal{V}(\vec{r}) \equiv \left(-\frac{4\pi}{3}a^{3}\right) k_{B} T(2\chi), \qquad (2.48)$$

to capture of the net effect of attractions, and such that 2

$$-\beta E_{att.} = N^2 \left(\frac{a}{R}\right)^3 \chi. \tag{2.49}$$

The resulting free energy, with R as a variational parameter,

$$\ln Z(N,R) = N \ln g - \frac{3}{2} \ln \left[\frac{4\pi N a \xi_p}{3} \right] - \frac{3R^2}{4N a \xi_p} - \frac{N^2}{2} \left(\frac{a}{R} \right)^3 - \frac{N^3}{6} \left(\frac{a}{R} \right)^6 - \dots + \chi N^2 \left(\frac{a}{R} \right)^3 , \qquad (2.50)$$

will next be used to explore the phases of the interacting homopolymer.

²In the lattice model, a very similar expression is obtained by setting $N_{mm}=N^2/2V$ in Eq. (2.43).

2.2.2 Swollen (coil) polymers in good solvents

Most of the terms in the trial free energy of Eq. (2.50) have definite sign. The exception is the term proportional to $N^2(a/R)^3$ which has opposing contributions from the repulsive and attractive parts of the potential, and is proportional to $(\chi - 1/2)$. The sign of this term determines whether attraction or repulsion is the dominant effect, leading to two different phases. For $\chi < 1/2$ repulsion is more important, favoring large R and swollen polymers. This tendency is opposed by the reduction of entropy at larger R. Indeed, one can self-consistently check that all other terms are less important in this limit, such that

$$\ln Z(N,R) = \text{constant} - \frac{3R^2}{4Na\xi_p} - \frac{1-2\chi}{2}N^2\left(\frac{a}{R}\right)^3 + \text{higher order terms.}$$
 (2.51)

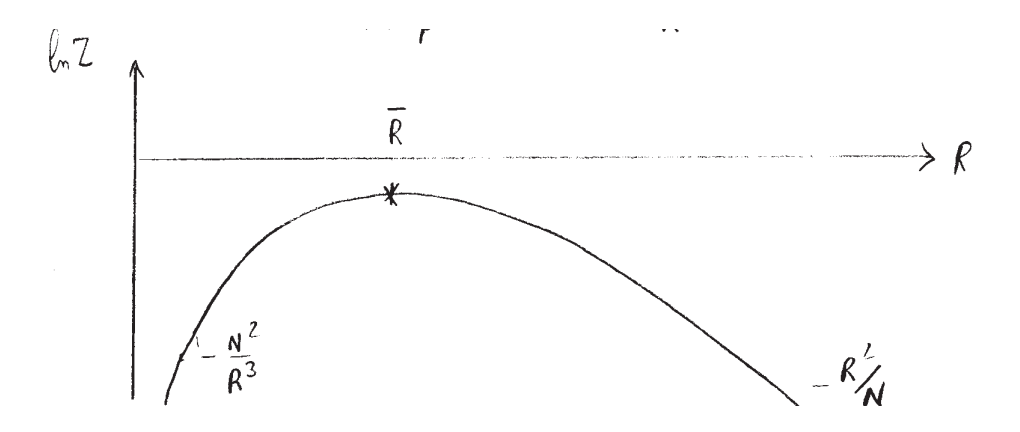


Figure 7: Variational free energy for a swollen polymer.

Extremizing the above expression leads to

$$\frac{\partial \ln Z}{\partial R} = -\frac{3R}{2Na\xi_p} + \frac{3(1-2\chi)}{2}N^2 \left(\frac{a^3}{R^4}\right) \Rightarrow \overline{R}^{5} = (1-2\chi)a^4\xi_p N^3,$$

$$\overline{R} = (1-2\chi)^{1/5} (a^4\xi_p)^{1/5} N^{3/5}.$$
(2.52)

In the absence of interactions, the typical size of the polymer grows as $\sqrt{a\xi_p N}$, as in Eq. (2.39). An important consequence of repulsion due to excluded volume is that the scaling of size is changed to $R \propto N^{\nu}$, with an exponent $\nu > 1/2$. The variational treatment leading to Eq. (2.52) thus predicts the so-called *Flory exponent* of $\nu = 3/5$.

Going beyond the mean-field variational treatment is not trivial, and one of the triumphs of renormalization group theory is to find the exact value of $\nu = 0.591...$, remarkably close to the Flory estimate of 3/5. While not directly relevant to real polymers, it is possible to inquire about the exponent ν for self-avoding walks in d-spatial dimensions—e.g., for polymers confined to a d=2 dimensional surface. Ignoring the attractive part of the interaction, but incorporating the repulsive cores, generalizes Eq. (2.51) to

$$\ln Z(N,R) = \text{constant} - \frac{dR^2}{4Na\xi_p} - \frac{N^2}{2} \left(\frac{a}{R}\right)^d. \tag{2.53}$$

Extremization now gives

$$\frac{\partial \ln Z}{\partial R} = -\frac{dR}{2Na\xi_p} + \frac{d}{2}N^2 \left(\frac{a^d}{R^{d+1}}\right) \ \Rightarrow \ \overline{R} = \left(a^{d+1}\xi_p\right)^{\frac{1}{d+2}} N^{\frac{3}{d+2}} \,,$$

leading to a generalized Flory exponent of

$$\nu_F(d) = \frac{3}{d+2} \,. \tag{2.54}$$

The predicted values of $\nu=1,\ 3/4,\ 1/2$ in $d=1,\ 2,\ 4$ are in fact exact. Above four dimensions the excluded volume constraint is unimportant as intersections of a random walk are asymptotically rare, and ν retains the random walk value of 1/2.

2.2.3 Compact (globular) polymers in bad solvents

On lowering temperature $\chi(T)$ typically becomes larger, and the coefficient $(1 - 2\chi)$ in Eq. (2.51) changes sign at the so-called θ -point (where $\chi(\theta) = 1/2$). At temperatures $T < \theta$ the attractive component of the interaction is more important, leading to compact (globular) shapes with a finite number density $\rho = N(a/R)^3$. The leading terms in the expansion of the variational free energy can now be recast as ³

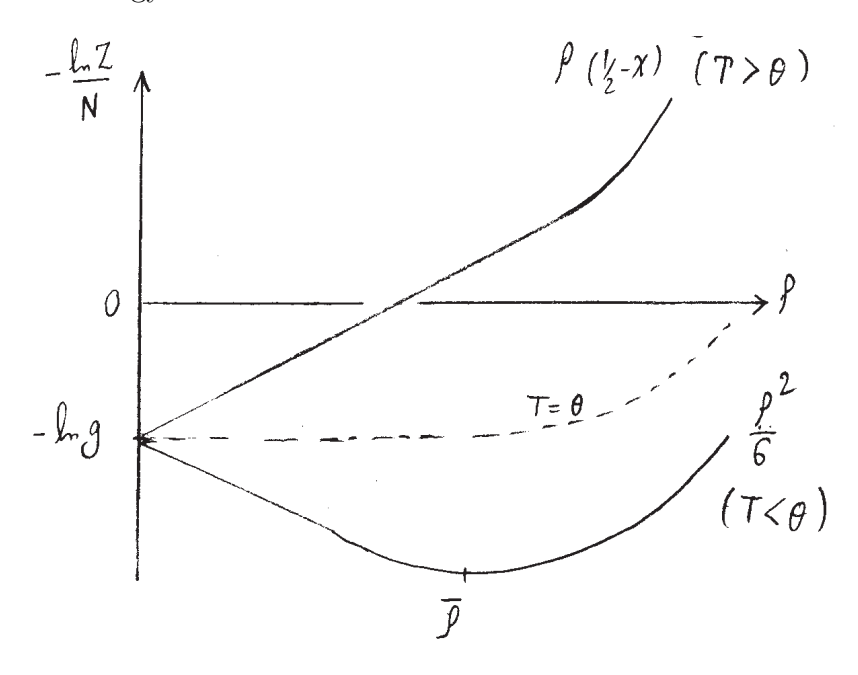


Figure 8: Variational free energy for a compact polymer.

$$-\frac{\ln Z(\rho)}{N} = -\ln g + \frac{1 - 2\chi}{2}\rho + \frac{\rho^2}{6} + \text{higher order terms.}$$
 (2.55)

³In the compact state, $R^3 \propto N$, the elastic term scales as $R^2/N \propto N^{-1/3}$, and is negligible for $N \gg 1$.

The optimal density for $T < \theta$ is obtained by minimizing the above free energy,

$$-\frac{1}{N}\frac{d\ln Z}{d\rho}\bigg|_{\rho=\overline{\rho}} = \left(\frac{1}{2} - \chi\right) + \frac{\overline{\rho}}{3} + \cdots,$$

leading to

$$\overline{\rho} = 3\left(\chi - \frac{1}{2}\right) + \cdots, \tag{2.56}$$

i.e. a density that vanishes linearly on approaching the θ -temperature from below. The higher order terms ensure that the density does not exceed the maximum value of unity in a fully compact state.

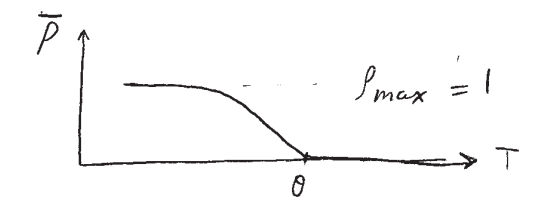


Figure 9: Variation of density in a compact polymer.

accounting for the reduction in free energy due to excluded volume.

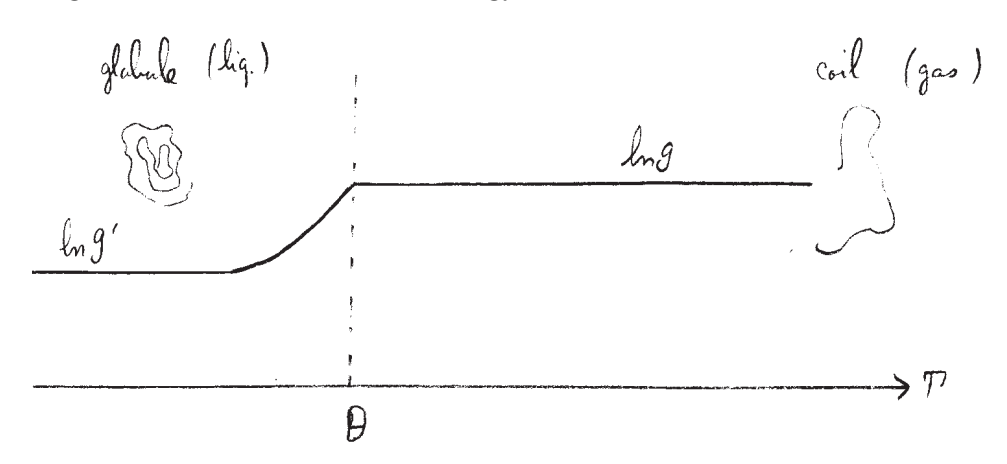


Figure 10: Variation of entropy in a compact polymer.

From Eq. (2.49) we note that the energy gain per particle from the attractive interactions satisfies

$$\frac{E_{att.}}{N} = -\overline{\rho}\chi k_B T. \tag{2.57}$$

From the construction of the partition function, it is further apparent that the entropy per particle is given by

$$\frac{S}{Nk_B} = \frac{-F + E}{Nk_B T} = \frac{\ln Z}{N} - \overline{\rho}\chi = \ln g + \frac{3}{2} \left(\chi - \frac{1}{2}\right)^2 + \dots - \overline{\rho}\chi \approx \ln g - \frac{\overline{\rho}}{2} - \frac{\overline{\rho}^2}{6} + \dots, \quad (2.58)$$

Thus close to the θ -temperature the entropy is reduced, initially linearly in temperature, although it also will eventually saturate as does the density. The above analysis is reminiscent of the mean-field analysis of the transition between a gas (low density) and a liquid (high density). The liquid state still encompasses many distinct configurations, although fewer than in a gas. Further cooling of liquids typically leads to frozen states with even lower entropy. We may thus inquire if such a freezing transition also exists for polymers.

2.2.4 Fractal Globule

In a dense globular state, excluded–volume interactions are effectively screened. One may then expect that subchains of length s behave approximately as ideal random walks, with spatial extent scaling as $R(s) \sim s^{1/2}$. Since the overall size of the globule scales as $R \sim N^{1/2}$, this random walk behavior must terminate at $s_{max} \sim N^{2/3}$ with $N^{1/3}$ such independent segments spanning the globule. The random walk behavior of these segments leads to a contact probability, see Eq.(2.40),

$$P(s) \sim \frac{1}{s^{3/2}}.$$

DNA fibers (chromatin) within the nucleus of a typical cell form a compact phase (characterized by a finite density). It is now possible to map out the probability that two segments of chromatin are in contact using the method of chromosome conformation capture (Hi–C). Surprising, these experiments suggests that over a wide range of genomic separations (hundreds of kilobases to a few megabases), the contact probability instead decays as

$$P(s) \sim \frac{1}{s}$$
.

This discrepancy suggests that chromatin is not organized as an equilibrated polymer globule of ideal subchains. Rather, it suggest to a different organization of the compact state that has been dubbed the **fractal (or crumpled) globule**.

The fractal globule, was in fact first proposed by Grosberg and collaborators, in the context of proteins, as a non-equilibrium conformation formed when a long polymer collapses rapidly without entanglement. Instead of fully mixing, the chain folds hierarchically into crumpled domains, each of which is segregated from others. This results in a self-similar, entanglement-free packing that fills space but preserves the territorial integrity of polymer segments. In this state, the scaling of subchain size is altered to $R(s) \sim s^{1/3}$, consistent with finite density, while the contact probability follows as $P(s) \sim s^{-1}$, (inversely in volume) as observed in chromatin.

The fractal globule model thus provides a possible explanation for experimental observations of chromatin folding. It suggests that the genome is organized into crumpled, metastable domains that minimize entanglement, thereby facilitating both efficient compaction and accessibility required for gene regulation. While over very long times an equilibrium globule may eventually be approached, the kinetics of topological relaxation are exceedingly slow, making the fractal globule a biologically relevant intermediate state.